Thermal Barrier Coating (TBC) of 8 Yttria Stabilized Zirconia and Mullite on Medium Carbon Steel

*M. S. F. Zaini, A.M. I. Mamat, J. B. Saedon, M. S. Adenan**
Faculty of Mechanical Engineering, Universiti Teknologi MARA,
40450 Shah Alam, Selangor, Malaysia
**mshahriman@uitm.edu.my*

ABSTRACT

Thermal barrier coating (TBC) usually is deposited on nickel-based superalloy substrates for high temperature applications. In this study however, TBC is deposited on medium carbon steel with two different topcoat material which are the 8 wt% yttria stabilized zirconia (8YSZ) and the mullite using an air plasma spraying (APS) method. The aim is to reduce the heat transfer in its application as thermal barriers in electrical turbocompounding systems. The microstructure and thermal cycle life of the as-sprayed TBC are investigated. From the SEM image, the 8YSZ and mullite coating is uniformly deposited on a medium carbon steel substrate. The lifetime of 8YSZ coating is higher than of the mullite coating at 64 cycles for the 8YSZ coating and 14 cycles for the mullite coating. Consequently, in using medium carbon steel as a substrate, the applicable topcoat material for TBC application is the 8YSZ rather than the mullite in terms of better thermal cycle life.

Keywords: *Thermal barrier coating, Air plasma spray, 8YSZ, Mullite*

Introduction

Thermal barrier coating (TBC) is widely used in extreme temperature applications such as in gas turbines and aircrafts in order to improve the efficiency of the engine when the temperature increases during operation due to its excellent thermal resistance [1], [2]. The TBC will protect and reduce the temperature of the metal substrate which will therefore extend the lifetime of the components. Other than that, TBC can also add to the resistance to oxidation and hot corrosion of its metal substrate [3], [4]. A TBC is a unique multi-layered system that makes TBC great in performance and features. The

ISSN 1823- 5514, eISSN 2550-164X
Received for review: 2019-05-27
Accepted for publication: 2019-07-02
Published: 2020-06-30

layers of TBC are ceramic top coat, metallic bond coat and a thermally grown oxide (TGO) [5], [6]. These layers are made of different materials with different functions within the TBC system. However, some literatures state that the substrate is also part of the TBC layers [7], [8].

There are numerous materials that can be used as a top coat for a TBC such as yttria stabilized zirconia (YSZ), mullite, alumina, CeO^2+YSZ, $La_2Zr_2O_7$, silicate, rare earth oxides, metal-glass composite, $Y_3Al_xFe_{5-x}O_{12}$, $SrZrO_3$ and $BaZrO_3$, lanthanum aluminates, $(Ca_{1-x}Mg_x)Zr_4(PO_4)_6$ and LaPO4 [9]. Out of all of these, the most common material used as the topcoat is YSZ due to its admirable properties. The YSZ with wt% of 7-8 is the typical material used for the TBC top coat which provides it with great performance [9]–[11].

The function of the ceramic top coat is to be a thermal insulation to the substrate because of the top coat material itself [12], [13]. While, the bond coat protects the substrate from oxidation and corrosion, it also functions as adherence between the top coat and the substrate [14], [15]. Besides that, the function of the bond coat is to reduce thermal expansion mismatch between the ceramic top coat and the substrate [16]. When the thermal barrier is operating, TGO forms between the top coat and bond coat to provide bonding between them and to slow down subsequent oxidation [17].

Usually, TBC is used to protect nickel-based superalloy substrates [18]. For this research study, the TBC is developed on medium carbon steel material in order to know the differences of TBC performances with different topcoat materials on medium carbon steel substrates. The selection of carbon steel as a substrate material is because of several reasons such that it is low cost, easy to be machined and have high strength [19]. In this paper, 8YSZ and mullite coating is prepared using an air plasma spraying (APS) method for TBC to be used in electrical turbo compounding systems where the morphology and thermal cycle life of TBCs are investigated in detail. Ultimately, besides TBCs being used in reducing heat for turbines, this TBC which is obtained through APS can be applied as a heat shield component in electrical turbo compounding systems.

Methodology

Medium carbon steel substrates (AISI 1050) with dimensions of 200 mm x 100 mm x 2 mm are used in this research to identify the thermal cycle life and morphology of TBCs with different topcoat materials. Before the coating process, the substrate materials are cleaned from undesirable residues like lubricant and impurities using thinner and then blasted using Al_2O_3 with a mix of mesh 16 and 24. The NiCoCrAlY bond coat with a nominal composition of Ni-23Co-17Cr-12Al-0.5Y (wt %) is fabricated onto the substrates with a thickness of 100 μm using the APS method. Then, the 8YSZ and mullite

topcoat are deposited onto the bond coat with 250 µm of thickness using the same method. The air plasma spraying parameters used are listed in Table 1.

Table 1: The parameters for spraying bond coat and topcoat

Items	Bond coat	Top coat
Current (A)	600	600
Powder feed rate (g/min)	30	25
Stand-off distance (mm)	140	90
Argon flow (slpm)	65	44
Hydrogen flow (slpm)	14	13

*slpm: standard liters per minute

The coated samples are cut into 15 mm x 5 mm to produce cross sections. The cross sections of the cut samples are then polished using the regular metallographic approach. The Optical Microscope (OM, Olympus BX60F) and Scanning Electron Microscope (SEM, Hitachi SU3500) are used to observe the coatings' cross-sectional microstructures. The thermal cycle life test is conducted using the modified MIL-STD 883 Method 1010. The sample of coated TBC are cut into 50 mm x 50 mm and heated in a hot furnace (Carbolite HTF3 ELP) at 900°C. The heating time for one cycle is 30 min. Then, the sample is removed from the furnace to be cooled down using an air compressor to room temperature for 25 minutes. The whole process is considered as one cycle. The sample is placed into a furnace to repeat the process until failure is detected and the thermal cyclic test stops.

Results and Discussion

The deposited TBC with different topcoat materials are shown in Figure 1. From general observations of Figure 1 (a), it clearly shows that the 8YSZ topcoat produced a white yellowish coating compared to the mullite topcoat in Figure 1 (b). The colour of the mullite topcoat is whiter than of the 8YSZ coating. In order to get an initial picture of how the microstructures of both TBC looks like, the OM is used to capture their microstructure images. From the OM images, the deposition of TBC with 8YSZ and mullite on medium carbon steel substrate looks quite uniform. However, the OM image is not exactly clear and detailed. Hence, SEM is used to capture the image of as-sprayed TBC microstructures with clear and detailed images since the SEM equipment can perform larger magnifications than the OM.

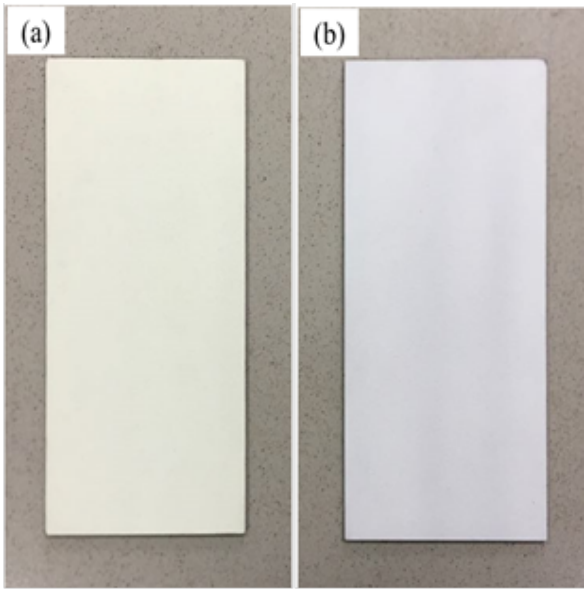

Figure 1: As-sprayed TBC with (a) 8YSZ top coat and (b) mullite top coat

The SEM image of the as-sprayed TBC with the 8YSZ and the mullite as top coats are shown in Figure 2 (a) and (b). The SEM result shows that the deposition of ceramic coating on medium carbon steel as a substrate is uniform with no cracks found. From the SEM image of the 8YSZ and mullite results, it clearly shows that the APS method produces lamellar microstructures [20]. The APS laminar structures are mostly more efficient for thermal insulation because the thermal conductivity is as low as 0.8 W/mk but it has less resistant towards in-plane cyclic mechanical loading [21]. While the Electron Beam-Physical Vapor Deposition (EB-PVD) method produces TBC with columnar microstructures [22]. The microstructure of 8YSZ and mullite TBCs that are deposited on the medium carbon steel substrate are the same as other researchers' outcome where the molecules melt and form grain boundaries in between [6].

From the SEM image, there is an appearance of unorganized micro-pores in the 8YSZ and mullite topcoat. This is a normal phenomenon for plasma-sprayed coating [5]. In addition, the presence of porosity inside the 8YSZ and mullite top coat can be beneficial since porosity is usually able to reduce the thermal conductivity value of the TBC and it can also boost the insulating efficiency of the TBC [5]. The SEM images of the 8YSZ and mullite samples with x500 magnification are shown in Figure 3. It clearly shows that there exist micro-pores within the coating layer that is deposited using the APS. From that SEM image, 8YSZ coating has a lot more pores compared to

mullite coating. This occurs due to the rapid hardening process of plasma splashing, the air breaks down within the liquid particles which floods the outside of the coatings and consequently frames the pores [23].

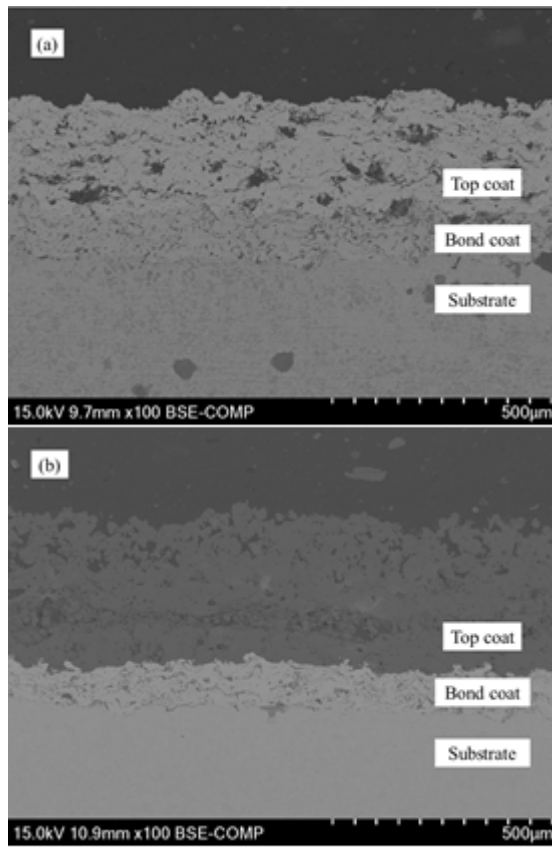

Figure 2: The microstructure image of TBC from SEM (a) 8YSZ, (b) mullite

From the SEM images in Figure 3 and Figure 4, it also shows that the surface of the topcoat, topcoat-bond coat interface and bond coat-substrate interface are rough. The roughness in the bond coat-substrate interface is formed because of the grit blasting process before the deposition process which can improve adherence and also increase its mechanical bonding between the coating and the substrate. While the roughness on the surface of the topcoat and the interface of the top coat-bond coat is formed because of the features of the APS itself. This is because the splats are stacked on top of each other during the APS process which results in layered coatings with high roughness [24].

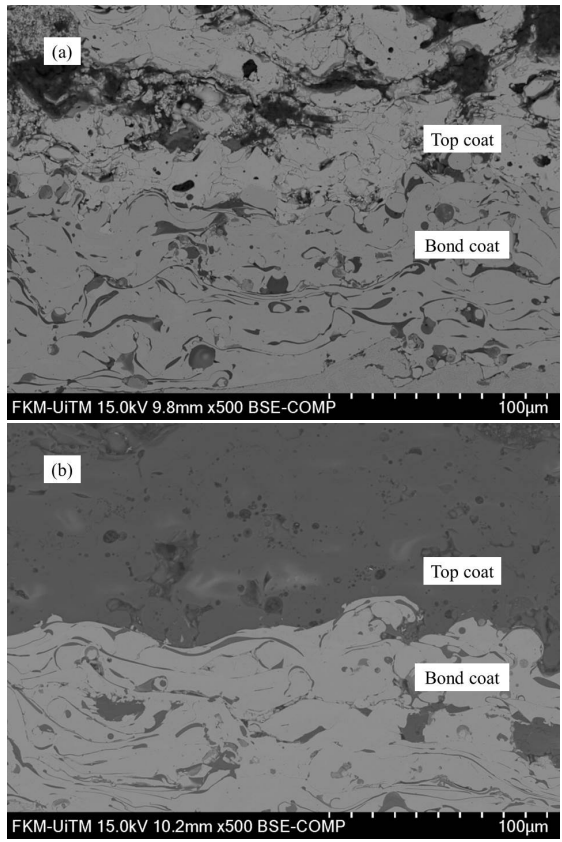

Figure 3: The SEM image of top coat/bond coat layer for (a) 8YSZ, (b) mullite

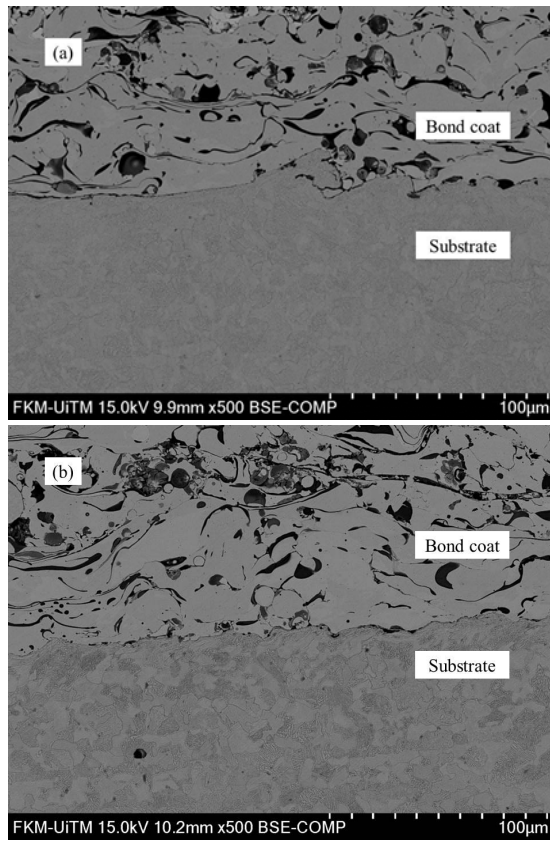

Figure 4: The SEM image of bond coat/substrate layer for (a) 8YSZ and (b) mullite

The condition of the 8YSZ and mullite top coat TBC samples after thermal cycle life test are shown in Figure 5. Failure happens in the 8YSZ top coat sample after 64 cycles. While the mullite sample failed just after 14 cycles. From these results, it clearly shows that lifetime of the 8YSZ top coat deposited on medium carbon steel is longer than the lifetime of the mullite top coat. The main failure mechanism of TBC while operating the system is driven by thermal expansion coefficient mismatch between ceramic coating and metallic substrate and also because of the TGO formation between the ceramic top coat and the bond coat interface [25]. A TGO coating is a layer that forms during operating and service of the TBC due to the oxidation of the bond coat. Both of these effects are the main impetus to nucleation, propagation and

coalescence of cracks parallel to the interface between the ceramic topcoat and the metallic bond coat that can cause the spallation of TBCs.

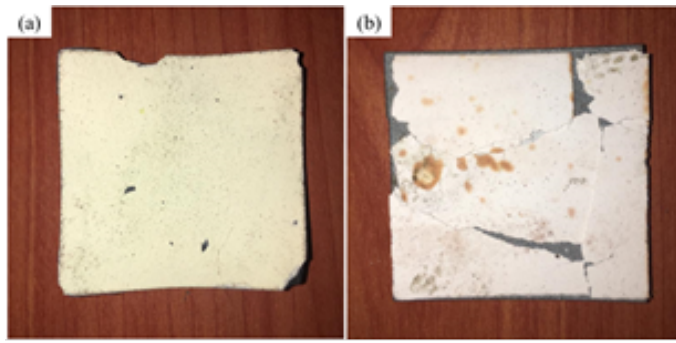

Figure 5: The sample of (a) 8YSZ and (b) mullite after thermal cycle life test

In this case, the TGO forms during the heating process of the sample. When the cycles keep repeating, the TGO thickness keeps on increasing. At cycles 14, the mullite coating could not hold the TGO effects which is when peel off occurs. On the other hand, the failure of the 8YSZ sample is not as bad as the mullite sample. The mullite coating with the bond coat totally peels off from the substrate. While the 8YSZ's coating is still attached to the substrate with only small parts of topcoat is peeled off. In order to increase the lifetime of the TBC system, the thickness of the TGO must be reduced. One of the best methods to reduce a TGO thickness is through a shot peening process. A shot peening method produces uniform TGO structures and lower oxide content compared to the APS method. This is because when the surface roughness is decreased, a lower TGO surface area and uniformity of TBC is gained [16].

Conclusion

As a conclusion, the 8YSZ and mullite topcoat is uniformly deposited on a medium carbon steel substrate. Besides that, the ceramic coating that is deposited using the APS method has micro-pores within its layers. The pores in the 8YSZ layers are more in numbers compared to the pores within the mullite layers. This porosity is good because it can reduce thermal conductivity of the TBC and can also boost the insulating efficiency of the TBC. In terms of thermal cycle life, the 8YSZ sample is better than the mullite sample. Because of its properties, YSZ with wt% of 7-8 is used as the typical material for topcoats in TBCs and can result in great performance of TBCs. Overall, medium carbon steel can be used as a TBC substrate, but it depends on the

application since TBC can be deposited on it. In addition, its performance is not good as the TBC deposited on nickel-based superalloy substrates.

References

[1] Y. Wang, J. Li, H. Liu, and Y. Weng, "Study on thermal resistance performance of 8YSZ thermal barrier coatings," *Int. J. Therm. Sci.*, vol. 122, pp. 12–25, 2017.

[2] L. Yang, H. L. Li, Y. C. Zhou, W. Zhu, Y. G. Wei, and J. P. Zhang, "Erosion failure mechanism of EB-PVD thermal barrier coatings with real morphology," *Wear*, vol. 392–393, no. January, pp. 99–108, 2017.

[3] H. Guo, Y. Cui, H. Peng, and S. Gong, "Improved cyclic oxidation resistance of electron beam physical vapor deposited nano-oxide dispersed b-NiAl coatings for Hf-containing superalloy," *Corros. Sci.*, vol. 52, no. 4, pp. 1440–1446, 2010.

[4] M. H. Li, X. F. Sun, S. K. Gong, Z. Y. Zhang, H. R. Guan, and Z. Q. Hu, "Phase transformation and bond coat oxidation behavior of EB-PVD thermal barrier coating," *Surf. Coat. Technol.*, vol. 176, pp. 209–214, 2004.

[5] H. R. Abedi, M. Salehi, and A. Shafyei, "Microstructural, mechanical and thermal shock properties of triple-layer TBCs with different thicknesses of bond coat and ceramic top coat deposited onto polyimide matrix composite," *Ceram. Int.*, vol. 44, no. 6, pp. 6212–6222, 2018.

[6] K. Torkashvand, E. Poursaeidi, and M. Mohammadi, "Effect of TGO thickness on the thermal barrier coatings life under thermal shock and thermal cycle loading," *Ceram. Int.*, no. December 2017, 2018.

[7] K. Jiang, S. Liu, and X. Wang, "Phase stability and thermal conductivity of nanostructured tetragonal yttria–stabilized zirconia thermal barrier coatings deposited by air–plasma spraying," *Ceram. Int.*, vol. 43, no. 15, pp. 12633–12640, 2017.

[8] N. P. Padture, "Thermal Barrier Coatings for Gas-Turbine Engine Applications," *Science (80-.).*, vol. 296, no. 5566, pp. 280–284, 2002.

[9] X. Q. Cao, R. Vassen, and D. Stoever, "Ceramic materials for thermal barrier coatings," *J. Eur. Ceram. Soc.*, vol. 24, no. 1, pp. 1–10, 2004.

[10] S. Barnwal and B. C. Bissa, "Thermal Barrier Coating System and Different Processes to apply them-A Review," *Int. J. Innov. Res. Sci. Eng. Technol. (An ISO Certif. Organ.*, vol. 3297, no. 9, pp. 8506–8512, 2007.

[11] H. Peng, L. Wang, L. Guo, W. Miao, H. Guo, and S. Gong, "Degradation of EB-PVD thermal barrier coatings caused by CMAS deposits," *Prog. Nat. Sci. Mater. Int.*, vol. 22, no. 5, pp. 461–467, 2012.

[12] J. Wang, J. Sun, H. Zhang, X. Zhou, L. Deng, and X. Cao, "Effect of spraying power on microstructure and property of nanostructured YSZ thermal barrier coatings," *J. Alloys Compd.*, vol. 730, pp. 471–482, 2018.

[13] J. Zhu and K. Ma, "Microstructural and mechanical properties of thermal barrier coating at 1400°C treatment," *Theor. Appl. Mech. Lett.*, vol. 4, no. 2, pp. 1–5, 2014.

[14] C. Nordhorn, R. Mücke, D. E. Mack, and R. Vaßen, "Probabilistic lifetime model for atmospherically plasma sprayed thermal barrier coating systems," *Mech. Mater.*, vol. 93, pp. 199–208, 2016.

[15] G. Mauer, D. Sebold, R. Vaßen, E. Hejrani, D. Naumenko, and W. J. Quadakkers, "Impact of processing conditions and feedstock characteristics on thermally sprayed MCrAlY bondcoat properties," *Surf. Coatings Technol.*, vol. 318, pp. 114–121, 2017.

[16] A. C. Karaoglanli, K. M. Doleker, B. Demirel, A. Turk, and R. Varol, "Effect of shot peening on the oxidation behavior of thermal barrier coatings," *Appl. Surf. Sci.*, vol. 354, pp. 314–322, 2015.

[17] R. Darolia, "Thermal barrier coatings technology: critical review, progress update, remaining challenges and prospects," *Int. Mater. Rev.*, vol. 58, no. 6, pp. 315–348, 2013.

[18] S. Gong and Q. Wu, "Processing, microstructures and properties of thermal barrier coatings by electron beam physical vapor deposition (EB-PVD)," *Therm. Barrier Coatings*, pp. 115–131, 2011.

[19] W. Yang, Q. Li, W. Liu, Z. Peng, B. Liu, and J. Liang, "Characterization of plasma electrolytic oxidation coating on low carbon steel prepared from silicate electrolyte with Al nanoparticles," *Ceram. Int.*, vol. 43, no. 18, pp. 16851–16858, 2017.

[20] Z. X. Yu, J. B. Huang, W. Z. Wang, J. Y. Yu, and L. M. Wu, "Deposition and properties of a multilayered thermal barrier coating," *Surf. Coatings Technol.*, vol. 288, pp. 126–134, 2016.

[21] Y. Liu, V. Vidal, S. Le Roux, F. Blas, F. Ansart, and P. Lours, "Influence of isothermal and cyclic oxidation on the apparent interfacial toughness in thermal barrier coating systems," *J. Eur. Ceram. Soc.*, vol. 35, no. 15, pp. 4269–4275, 2015.

[22] M. S. Sahith, G. Giridhara, and R. S. Kumar, "Development and analysis of thermal barrier coatings on gas turbine blades - A Review," *Mater. Today Proc.*, vol. 5, no. 1, pp. 2746–2751, 2018.

[23] F. Zhou, Y. Wang, L. Wang, Z. Cui, and Z. Zhang, "High temperature oxidation and insulation behavior of plasma-sprayed nanostructured thermal barrier coatings," *J. Alloys Compd.*, vol. 704, pp. 614–623, 2017.

[24] R. Ghasemi and H. Vakilifard, "Plasma-sprayed nanostructured YSZ thermal barrier coatings: Thermal insulation capability and adhesion strength," *Ceram. Int.*, vol. 43, no. 12, pp. 8556–8563, 2017.

[25] F. Cernuschi *et al.*, "Solid particle erosion of thermal spray and physical vapour deposition thermal barrier coatings," *Wear*, vol. 271, no. 11–12, pp. 2909–2918, 2011.